

Persistence of Coherent Quantum Dynamics at Strong Dissipation

Denis Kast and Joachim Ankerhold

Institut für Theoretische Physik, Universität Ulm, Albert-Einstein-Allee 11, 89069 Ulm, Germany

(Received 18 April 2012; published 2 January 2013)

The quantum dynamics of a two-state system coupled to a bosonic reservoir with sub-Ohmic spectral density is investigated for strong friction. Numerically exact path integral Monte Carlo methods reveal that a changeover from coherent to incoherent relaxation does not occur for a broad class of spectral distributions. In nonequilibrium coherences associated with substantial system-reservoir entanglement exist even when strong dissipation forces the thermodynamic state of the system to behave almost classically. This may be of relevance for current experiments with nanoscale devices.

DOI: [10.1103/PhysRevLett.110.010402](https://doi.org/10.1103/PhysRevLett.110.010402)

PACS numbers: 03.65.Yz, 03.67.-a, 05.10.Ln, 73.63.-b

Introduction.—The impact of dissipative environments on the dynamics of quantum systems has regained interest due to the boost of activities to tailor atomic, molecular, and solid state structures with growing complexity [1–3]. Common wisdom is that quantum coherence is inevitably destroyed at sufficiently strong coupling to broadband reservoirs. A paradigmatic model is a two-state system interacting with a reservoir of bosonic degrees of freedom (spin-boson model), which plays a fundamental role in a variety of applications [4–6]. At low temperatures and weak coupling, an initial nonequilibrium state evolves via damped coherent oscillations, while at stronger dissipation it displays an incoherent decay toward thermal equilibrium. This is often understood as a quantum to classical changeover. The question we pose here is whether this picture always applies.

The spin-boson (SB) model has recently gained renewed attention for reservoirs with sub-Ohmic mode distributions $J_s(\omega) \propto \alpha \omega^s$ where α denotes a coupling constant and $0 < s < 1$. This class of reservoirs constitutes a dominant noise source in solid state devices at low temperatures such as superconducting qubits [7] and quantum dots [8] with the spectral exponent s determined by the microscopic nature of environmental degrees of freedom. It also appears in the context of ultraslow glass dynamics [9], quantum impurity systems [10], and nanomechanical oscillators [11]. Advanced numerical techniques [12–15] have revealed that at zero temperature the equilibrium state exhibits at a critical coupling strength α_c a quantum phase transition (QPT) from a delocalized phase with tunneling between the two spin orientations (weak friction) to a localized one with almost classical behavior (stronger friction) [16].

The time evolution of the polarization toward these asymptotic phases shows coherent oscillations or classical-like monotonic decay. It has been argued that with increasing friction the relaxation dynamics *always* turns from coherent to incoherent [17]. Indeed, numerical studies [18] confirmed this picture for reservoirs with $1/2 \leq s < 1$, but the situation for $0 < s < 1/2$ remained unclear, mainly because approaches used previously are

restricted to the regime of weak to moderate dissipation [12,19]. The goal of this Letter is to attack this latter regime via real-time path integral Monte Carlo (PIMC) techniques [20,21], which also cover strong friction. We verify that coherences persist in nonequilibrium for arbitrary coupling strength to a heat bath even when the thermal state is essentially classical. Our results shed new light on our understanding of the quantum–classical crossover and may be accessible experimentally.

Reduced dynamics.—We consider a symmetric SB model

$$H_{\text{SB}} = -\frac{\hbar\Delta}{2}\sigma_x - \frac{1}{2}\sigma_z\mathcal{E} + \sum_{\alpha}\hbar\omega_{\alpha}b_{\alpha}^{\dagger}b_{\alpha} \quad (1)$$

with a two-state system (TSS) that interacts bilinearly with a harmonic reservoir H_B via the bath force $\mathcal{E} = \sum_{\alpha}\lambda_{\alpha}(b_{\alpha} + b_{\alpha}^{\dagger})$. All relevant observables are obtained from the reduced density operator $\rho(t) = \text{Tr}_B\{\exp(-iH_{\text{SB}}t/\hbar)W(0)\exp(iH_{\text{SB}}t/\hbar)\}$, where the initial state has the form

$$W(0) = \rho_S(0)e^{-\beta(H_B - \mathcal{E})}/Z_B. \quad (2)$$

Here, according to typical experimental situations [5] the bath distribution is equilibrated to the initial state of the TSS, which is $\rho_S(0) = | + 1\rangle\langle + 1|$ (the eigenstates of σ_z are $|\pm 1\rangle$ with the bare tunneling amplitude Δ between them); the partition function is denoted by Z_B . We are interested in the real-time dynamics of the observables

$$P_{\nu}(t) \equiv \langle \sigma_{\nu}(t) \rangle = \text{Tr}\{\sigma_{\nu}\rho(t)\}, \quad \nu = x, y, z,$$

where P_z describes the population difference (polarization) and P_x the coherence between the sites $|\pm 1\rangle$.

A nonperturbative treatment is obtained within the path integral formulation. The P_{ν} is expressed along a Keldysh contour with forward σ and backward σ' paths [5]. The impact of the environment appears as an influence functional introducing arbitrarily long-ranged interactions between the paths. Switching to $\eta/\xi = \sigma \pm \sigma'$ one arrives at

$$P_\nu(t) = \int \mathcal{D}[\eta] \mathcal{D}[\xi] \mathcal{A}_\nu e^{-\Phi[\eta, \xi]} \quad (3)$$

with the contribution \mathcal{A}_ν in the absence of dissipation and the influence functional

$$\begin{aligned} \Phi[\eta, \xi] = & \int_0^t du \int_0^u dv \dot{\xi}(u) [Q'(u-v)\dot{\xi}(v) \\ & + iQ''(u-v)\dot{\eta}(v)]. \end{aligned}$$

According to Eq. (2) one sums over all paths with $\eta(0) = 1$, $\xi(0) = 0$ and $|\eta(t)| = 1$, $\xi(t) = 0$ for P_z and $\eta(t) = 0$, $|\xi(t)| = 1$ for P_x , respectively. The kernel $Q = Q' + iQ''$ is related to the bath correlation $\dot{Q}(t) = \langle \mathcal{E}(t)\mathcal{E}(0) \rangle / \hbar^2$ and is thus completely determined by the spectral function $J(\omega) = \pi \sum_\alpha \lambda_\alpha^2 \delta(\omega - \omega_\alpha)$. For sub-Ohmic spectral distributions

$$J_s(\omega) = 2\pi\alpha\omega_c^{1-s}\omega^s e^{-\omega/\omega_c}, \quad 0 < s < 1, \quad (4)$$

one has at zero temperature [5]

$$Q_0(t) = 2\alpha\Gamma(s-1)[1 - (1 + i\omega_c t)^{1-s}].$$

In the Ohmic case $s \rightarrow 1$ the coupling α coincides with the Kondo parameter K . The cutoff ω_c corresponds, e.g., to a Debye frequency [5] or to a parameter of an electromagnetic environment [8].

A direct evaluation of Eq. (3) is extremely challenging due to the retardation in the influence functional, which grows with decreasing temperature. In this situation PIMC methods are a very powerful means to explore the non-perturbative range including strong coupling [20,21]. Here, we extend this formulation to simulate not only populations P_z but also coherences P_x (see Ref. [22]).

Population dynamics.—The dynamics of $P_z(t)$ directly displays the impact of decoherence as the bare two-state system is completely quantum and has no classical limit. The expectation is that finite friction induces damped oscillations on a transient time scale of the form $P_z(t) \sim e^{-\gamma t} \cos(\Omega t)$. As long as $\Omega \neq 0$ the system dynamics is said to be coherent; otherwise it is incoherent. For vanishing friction $P_z(t) = \cos(\Delta t)$, while finite coupling leads asymptotically to a thermal equilibrium with $P_z(t \rightarrow \infty) \rightarrow 0$ (delocalized) or $P_z(t \rightarrow \infty) \neq 0$ (localized) as shown previously [12,13].

To analyze the dynamical features in detail (cf. Fig. 1), we consider the case of zero temperature and $\omega_c \gg \Delta$, and start in Fig. 2 with $P_z(t)$ in the range $1/2 \leq s \leq 1$ of spectral exponents. For fixed s , PIMC simulations display with increasing coupling α a changeover from coherent to incoherent motion, i.e., from damped oscillations to overdamped decay [18]. It appears in that domain in parameter space where the thermal state is delocalized (Fig. 1). Accordingly, the critical coupling strength for the coherent-incoherent turnover $\alpha_{CI}(s)$ is always smaller than the critical coupling $\alpha_c(s)$ for the QPT. In limiting cases one finds $\alpha_c(s = 0.5) \approx \alpha_{CI}(s = 0.5)$, while for an

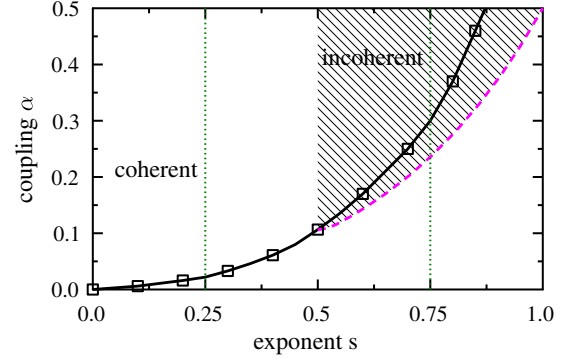


FIG. 1 (color online). Domains of coherent (white) and incoherent (shaded) dynamics of the SB model for a sub-Ohmic environment (4) at zero temperature. Above (below) the solid line $\alpha_c(s)$ the system asymptotically reaches a thermal equilibrium that is localized (delocalized) [27]. A coherent-incoherent changeover only occurs along the dashed line $\alpha_{CI}(s)$ (2). Dotted lines refer to results in Fig. 2 (left) and Fig. 3 (right), respectively.

Ohmic bath ($s = 1$) the known result is confirmed $\alpha_c(s = 1) \approx 1 > \alpha_{CI}(s = 1) \approx 0.5$.

In contrast, simulations in the range $0 < s < 1/2$ reveal a different scenario. Oscillatory patterns survive even for coupling strengths far beyond the critical coupling $\alpha_c(s)$ for the QPT (see Figs. 1 and 3). PIMC data up to ultra-strong couplings $\alpha = 30\alpha_c$ do not show a changeover to a classical-like decay for exponents up to $s = 0.49$. The oscillation frequencies $\Omega_s(\alpha)$ in $P_z(t)$ increase with increasing coupling and exhibit a scale invariance according to $\Omega_s(\kappa\alpha) = \kappa\Omega_s(\alpha)$ (inset Fig. 3 and Ref. [22]). Two observations are intriguing: (i) even in the regime where friction is so strong that the thermal state resides in the classical phase [13,15] (spin almost frozen with $P_z \sim 1 \gg P_x$), the nonequilibrium dynamics of the TSS preserves quantum coherence and (ii) the domain where these

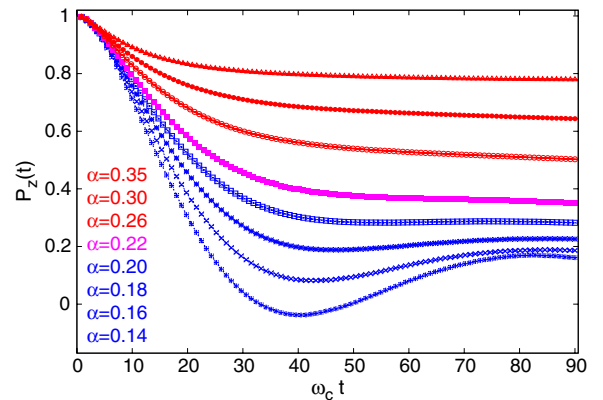


FIG. 2 (color online). Dynamics of $P_z(t)$ at $T = 0$ and $\Delta/\omega_c = 0.1$ according to PIMC calculations for $s = 0.75$ and couplings α with $\alpha_c \approx 0.3 > \alpha_{CI} \approx 0.22$ (purple line). Blue (red) lines refer to coherent ($\alpha < \alpha_{CI}$) (incoherent $\alpha > \alpha_{CI}$) dynamics (cf. Fig. 1). Statistical errors are of the size of the symbols.

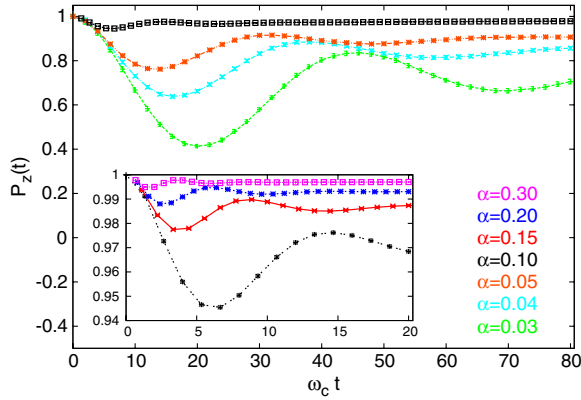


FIG. 3 (color online). Same as in Fig. 2 but for $s = 0.25$ and values $\alpha > \alpha_c \approx 0.022$. The inset shows a blowup for very large couplings.

coherences survive covers a broad range of spectral distributions up to exponents s close to $s = 0.5$ (see Fig. 1).

To gain analytical insight, an approximate treatment is provided by the noninteracting blip approximation (NIBA) [5]. The starting points are exact equations of motion that can be derived from (3) in Ref. [5], i.e.,

$$\dot{P}_z(t) = - \int_0^t du K_z(t-u) P_z(u). \quad (5)$$

Within NIBA the kernel is evaluated as $K_z \approx K_{N,z}$ where

$$K_{N,z}(t) = \Delta^2 e^{-Q'(t)} \cos[Q''(t)]. \quad (6)$$

Let us now analyze how incoherent decay for $P_z(t)$ may appear out of Eq. (5). In $K_{N,z}(t)$ the correlation $Q'_0(t)$ induces damping while $Q''_0(t)$ is responsible for oscillatory motion. Both functions are positive and monotonically increase in time leading to damped oscillations in $K_{N,z}(t)$. If this damping is sufficiently strong on the time scale of the bare dynamics $1/\Delta$, i.e., if the kernel is sufficiently short ranged in time, the population $P_z(t)$ decays incoherently. We estimate this to be the case if at the first zero $t = t_*$ of the kernel where $Q''_0(t_*) = \pi/2$, the damping obeys $Q'_0(t_*) > 1$. One finds this condition to be fulfilled only for $s > 1/2$. There, the borderline between the two dynamical regimes is determined by that coupling strength at which $t_* = 1/\Delta$, i.e.,

$$\alpha_{\text{CI}}(s) \approx \frac{\pi}{4|\Gamma(s-1)| \cos(s\pi/2)} \left(\frac{\Delta}{\omega_c}\right)^{1-s}. \quad (7)$$

This expression includes the known Ohmic result $\alpha_{\text{CI}}(s=1) = 0.5$ and captures accurately numerical data from our PIMC calculations. Further, it confirms our numerical finding that $\alpha_c(s) \geq \alpha_{\text{CI}}(s)$ (see Fig. 1). For fixed $s > 0.5$, increasing friction first destroys coherent dynamics before it also asymptotically induces localization. In contrast, for spectral functions $0 < s < 0.5$, a coherent-incoherent changeover never appears.

In principle, the oscillation frequency Ω_s and the damping γ_s of $P_z(t)$ can be extracted as complex-valued poles from the Laplace transform of Eq. (5), i.e., $\hat{P}(\lambda) = 1/[\lambda + \hat{K}_{N,z}(\lambda)]$. However, specific results can be found only for (i) $s = 0.5$ and (ii) $s \ll 1$ (for details see Ref. [22]).

(i) In the regime $\alpha \ll \sqrt{\Delta/\omega_c}$, the poles are given by $\lambda_{1/2}^{\pm} = \pm i\Omega_{1/2} - \gamma_{1/2}$ with frequency $\Omega_{1/2}(\alpha) \approx \Delta - \gamma_{1/2}$ and decay rate $\gamma_{1/2}(\alpha) = \alpha\Delta\pi\sqrt{\omega_c/4\Delta}$. There is no pole with $\lambda = 0$ meaning that $P_z(t \rightarrow \infty) \rightarrow 0$ (delocalization). Apparently, the oscillation frequency *decreases* with growing coupling α while the damping rate *increases*. This indicates a changeover from coherent motion with $\Omega_{1/2}/\gamma_{1/2} > 1$ to incoherent motion with $\Omega_{1/2} = 0$ for larger α .

(ii) In the domain $s \ll 1$ one may use the expansion $Q_0(t) \approx \Lambda_s t \exp[i\pi(1-s)/2]$ with coefficient $\Lambda_s = \int_0^\infty d\omega J_s(\omega)/(\pi\omega) = 2\alpha\omega_c|\Gamma(s-1)|$. Then, $\hat{P}(\lambda)$ has one pole at $\lambda = 0$ so that $P_z(t)$ relaxes toward an asymptotic limit $P_z(t \rightarrow \infty) > 0$ (localization). The other two poles are complex conjugates where the imaginary part describes oscillations in $P_z(t)$ with frequency

$$\Omega_s(\alpha) \approx \Lambda_s \sin[(1-s)\pi/2] \approx \frac{2\alpha\omega_c}{s}. \quad (8)$$

The real part corresponds to a damping rate $\gamma_s(\alpha) \approx s\Lambda_s$ which saturates for $s \rightarrow 0$ at $\gamma_0 = 2\alpha\omega_c$. Hence, for fixed s , both rate and frequency *increase* with *increasing* α such that the dynamics of the TSS is always underdamped $\Omega_s/\gamma_s = 1/s \gg 1$. Quantum coherent dynamics persists up to arbitrarily large couplings in accordance with the numerical data (cf. Fig. 3). Further, the above result confirms the scaling property of $\Omega_s(\alpha)$ found already in the PIMC calculations. Note that details of the cutoff procedure may enter via Λ_s only. Because it is determined by the low frequency behavior of $J(\omega)$, the dynamics is independent of the cutoff scheme for $\omega_c \gg \Delta$ as also seen in the PIMC calculations (not shown). Similarly, the bare frequency of the TSS has disappeared. It only governs the dynamics for ultrashort times $t \ll 1/\omega_c$ before reservoir modes can respond. There, the bare Schrödinger dynamics predicts the universal quadratic time dependence $P_z(t) \approx 1 - \Delta^2 t^2/2$. After this initial delocalization process, the reservoir tends to prevail with the low frequency modes in \mathcal{E} [see Eq. (1)] acting on the TSS effectively as a static energy bias of strength $-\hbar\Lambda_s$ according to the coupling $-\sigma_z \mathcal{E}/2$. This is in agreement with the observation that $\hbar\Lambda_s$ corresponds to the energy needed to reorganize the reservoir once the spin has flipped [23].

Coherences and entanglement.—To further verify the quantum nature of the oscillatory population dynamics, we also monitor $P_x(t)$ (Fig. 4). Indeed, one observes substantial quantum nonlocality, which also suggests substantial entanglement between the TSS and its surroundings. At $T = 0$ this entanglement can be extracted from the von Neumann entropy $S(t)/k_B = -w_+ \ln(w_+) - w_- \ln(w_-)$

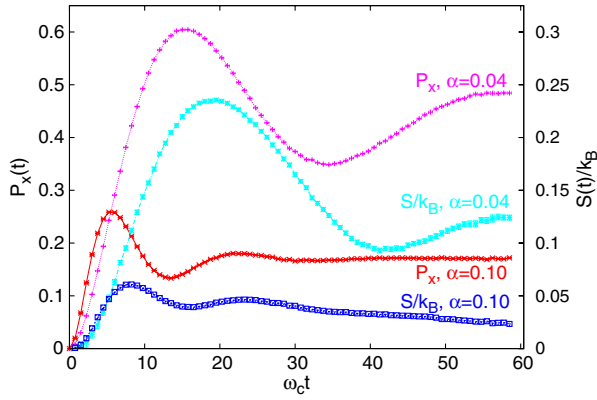


FIG. 4 (color online). Coherences $P_x(t)$ (left axis) and entropy $S(t)$ (right axis) for $s = 0.25$ ($\alpha_c \approx 0.022$) at $T = 0$ according to PIMC calculations.

with $w_{\pm} = \frac{1}{2}[1 \pm \sqrt{P_x(t)^2 + P_y(t)^2 + P_z(t)^2}]$ (cf. Fig. 4). PIMC simulations reveal strong entanglement well into the regime $\alpha > \alpha_c$ (localization) on time scales where oscillatory patterns in $P_z(t)$ and $P_x(t)$ occur. For longer times and stronger coupling, entanglement decays monotonically. This is in agreement with previous findings in thermal equilibrium: entanglement tends to zero in the localized phase for couplings somewhat above α_c [15].

Initial preparation.—Persistence of coherence is associated with a strong dependence on initial preparations. Of particular interest for experimental realizations are preparations, where the reservoir is out of equilibrium with respect to the initial state of the TSS. This means that in Eq. (2) one must replace $\mathcal{E} \rightarrow \mu\mathcal{E}$ with $\mu \neq 1$. The cloud of bath modes is shifted to the left (right) for $\mu < 1$ ($\mu > 1$) with $\mu = 0$ being the equilibrium orientation of the bare bath. According to Fig. 5, with decreasing μ the effective oscillations frequency of the TSS decreases while at the same time the initial loss in population increases. This behavior can be understood from the fact that this preparation can equivalently be described by a time dependent bias $\epsilon_{\mu}(t) = (1 - \mu)\dot{Q}''(t)$ of the TSS, i.e., by an additional term $\hbar\epsilon_{\mu}(t)\sigma_z/2$ in Eq. (1) [24]. In particular, for reservoirs with spectral exponents $s \ll 1$ one has $\dot{Q}''(t) \approx \Lambda_s$ so that $\epsilon_{\mu} \approx (1 - \mu)\Lambda_s$ becomes static. Effectively, this bias adds to the bias induced by the sluggish modes in the system-reservoir coupling $-\mathcal{E}\sigma_z/2$ [see below Eq. (8)] to produce a net bias $\epsilon_{\text{tot}} \approx -\mu\Lambda_s$. As a result the TSS regains bare dynamical features for $\mu \rightarrow 0$. This analysis can now be extended to other preparations of the TSS alone (superpositions of $|\pm 1\rangle$) which, however, display qualitatively a similar picture. The same is true for asymmetric TSS and/or finite temperatures as long as corresponding energy scales do not exceed the bare tunneling amplitude. Results will be shown elsewhere.

Summary.—We have shown that in nonequilibrium coherent dynamics can persist for ultrastrong coupling to a broadband reservoir. For a SB model in the sub-Ohmic

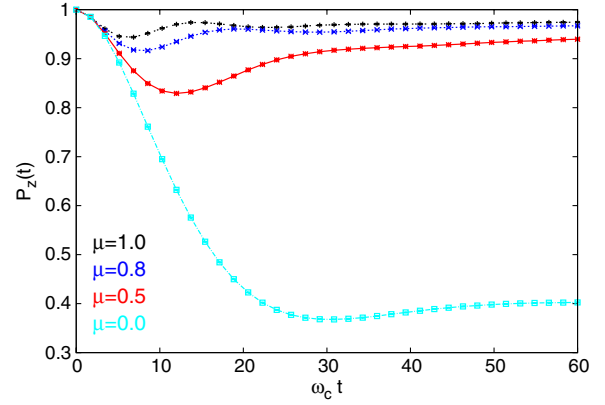


FIG. 5 (color online). $P_z(t)$ at $s = 0.25$, $\alpha = 0.1$ for various initial preparations of the reservoir with $\omega_c/\Delta = 10$. See text for details.

regime, stronger friction does not induce incoherent relaxation for spectral exponents $0 < s < 1/2$ even when the thermal equilibrium is almost classical. These findings shed light on our understanding of decoherence in open quantum systems and are thus of relevance for current experiments in nanoscale structures. The case $s = 1/2$ can be realized through a charge qubit subject to electromagnetic noise [8], while recent progress in engineering local environments for Cooper pair boxes may allow us to study cases with $s < 1/2$ [25]. Reservoirs with $s \rightarrow 0$ have been proposed as models for $1/f$ noise in superconducting circuits where temperature enters as an effective parameter [7]. While in this latter case details need to be investigated, a promising alternative is trapped ion systems as shown in Ref. [26].

We thank C. Escher, R. Bulla, A. Chin, H. Grabert, and M. Grifoni for valuable discussions. Financial support from the DFG through the SFB/TRR21 and the GIF is gratefully acknowledged.

-
- [1] B. Lanyon, C. Hempel, D. Nigg, M. Müller, R. Gerritsma, F. Zähringer, P. Schindler, J.T. Barreiro, M. Rambach, G. Kirchmair, M. Hennrich, P. Zoller, R. Blatt, and C.F. Roos, *Science* **334**, 57 (2011).
 - [2] Y. Kubo *et al.*, *Phys. Rev. Lett.* **107**, 220501 (2011).
 - [3] R. Hildner, D. Brinks, and N.F. van Hulst, *Nat. Phys.* **7**, 172 (2011).
 - [4] A.J. Leggett, S. Chakarvarty, A.T. Dorsey, M.P.A. Fisher, A. Garg, and W. Zwerger, *Rev. Mod. Phys.* **59**, 1 (1987).
 - [5] U. Weiss, *Quantum Dissipative Systems* (World Scientific, Singapore, 2008).
 - [6] H.P. Breuer and F. Petruccione, *The Theory of Open Quantum Systems* (Oxford University Press, Oxford, 2002).
 - [7] A. Shnirman, Y. Makhlin, and G. Schön, *Phys. Scr.* **T102**, 147 (2002).
 - [8] N.-H. Tong and M. Vojta, *Phys. Rev. Lett.* **97**, 016802 (2006).

- [9] D. Rosenberg, P. Nalbach, and D. D. Osheroff, *Phys. Rev. Lett.* **90**, 195501 (2003).
- [10] Q. Si, S. Rabello, K. Ingersent, and J.L. Smith, *Nature (London)* **413**, 804 (2001); P. Gegenwart, T. Westerkamp, C. Krellner, Y. Tokiwa, S. Paschen, C. Geibel, F. Steglich, E. Abrahams, and Q. Si, *Science* **315**, 969 (2007).
- [11] C. Seoanez, F. Guinea, and A.H. Castro Neto, *Europhys. Lett.* **78**, 60002 (2007).
- [12] F.B. Anders, R. Bulla, and M. Vojta, *Phys. Rev. Lett.* **98**, 210402 (2007).
- [13] A. Winter, H. Rieger, M. Vojta, and R. Bulla, *Phys. Rev. Lett.* **102**, 030601 (2009).
- [14] A. Alvermann and H. Fehske, *Phys. Rev. Lett.* **102**, 150601 (2009).
- [15] K. Le Hur, P. Doucet-Beaupré, and W. Hofstetter, *Phys. Rev. Lett.* **99**, 126801 (2007).
- [16] A. W. Chin, J. Prior, S. F. Huelga, and M. B. Plenio, *Phys. Rev. Lett.* **107**, 160601 (2011).
- [17] Q. Wang, A.-Y. Hu, and H. Zheng, *Phys. Rev. B* **80**, 214301 (2009).
- [18] P. Nalbach and M. Thorwart, *Phys. Rev. B* **81**, 054308 (2010).
- [19] H. Wang and M. Thoss, *Chem. Phys.* **370**, 78 (2010).
- [20] R. Egger and C.H. Mak, *Phys. Rev. B* **50**, 15210 (1994).
- [21] L. Mühlbacher and J. Ankerhold, *J. Chem. Phys.* **122**, 184715 (2005); L. Mühlbacher, J. Ankerhold, and A. Komnik, *Phys. Rev. Lett.* **95**, 220404 (2005).
- [22] See Supplemental Material at <http://link.aps.org/supplemental/10.1103/PhysRevLett.110.010402> for details on the analytical treatment in the range $s < 1/2$ and on the implementation of the measurement operator for σ_x in the PIMC scheme.
- [23] M. Thoss, H. Wang, and W.H. Miller, *J. Chem. Phys.* **115**, 2991 (2001).
- [24] A. Lucke, C.H. Mak, R. Egger, J. Ankerhold, J. Stockburger, and H. Grabert, *J. Chem. Phys.* **107**, 8397 (1997).
- [25] P. Solinas, M. Möttönen, J. Salmilehto, and J.P. Pekola, *Phys. Rev. B* **82**, 134517 (2010).
- [26] D. Porras, F. Marquardt, J. von Delft, and J.I. Cirac, *Phys. Rev. A* **78**, 010101(R) (2008).
- [27] Data points for the quantum phase transition are taken from Ref. [13].